A crystallographic study of Cys69Ala flavodoxin II from Azotobacter vinelandii: Structural determinants of redox potential

Alagaratnam, S.; van Pouderoyen, G; Pijning, T.; Dijkstra, B.W.; Cavazzini, D.; Rossi, G.L.; Van Dongen, W.M.A.M.; Van Mierlo, C.P.M.; Canters, G.W.; Van Berkel, WJH

Published in:
Protein Science

DOI:
10.1110/ps.051582605

A crystallographic study of Cys69Ala flavodoxin II from *Azotobacter vinelandii*: Structural determinants of redox potential

SHARMINI ALAGARATNAM,[1] GERTIE VAN POUDEROYEN,[2] TJAARD PIJNING,[2] BAUKE W. DIJKSTRA,[2] DAVIDE CAVAZZINI,[3] GIAN LUIGI ROSSI,[3] WALTER M.A.M. VAN DONGEN,[4] CARLO P.M. VAN MIERLO,[4] WILLEM J. H. VAN BERKEL,[4] AND GERARD W. CANTERS[1]

[1]Leiden Institute of Chemistry, Leiden University, 2300 RA Leiden, The Netherlands
[2]Laboratory of Biophysical Chemistry, University of Groningen, 9747 AG Groningen, The Netherlands
[3]Department of Biochemistry and Molecular Biology, University of Parma, Italy
[4]Laboratory of Biochemistry, Department of Agrotechnology and Food Sciences, Wageningen University, 6703 HA Wageningen, The Netherlands

(RECEIVED May 10, 2005; FINAL REVISION June 22, 2005; ACCEPTED June 23, 2005)

Abstract

Flavodoxin II from *Azotobacter vinelandii* is a "long-chain" flavodoxin and has one of the lowest E_1 midpoint potentials found within the flavodoxin family. To better understand the relationship between structural features and redox potentials, the oxidized form of the C69A mutant of this flavodoxin was crystallized and its three-dimensional structure determined to a resolution of 2.25 Å by molecular replacement. Its overall fold is similar to that of other flavodoxins, with a central five-stranded parallel β-sheet flanked on either side by α-helices. An eight-residue insertion, compared with other long-chain flavodoxins, forms a short 3_{10} helix preceding the start of the α_3 helix. The flavin mononucleotide (FMN) cofactor is flanked by a leucine on its *re* face instead of the more conserved tryptophan, resulting in a more solvent-accessible FMN binding site and stabilization of the hydroquinone (hq) state. In particular the absence of a hydrogen bond to the N5 atom of the oxidized FMN was identified, which destabilizes the ox form, as well as an exceptionally large patch of acidic residues in the vicinity of the FMN N1 atom, which destabilizes the hq form. It is also argued that the presence of a Gly at position 58 in the sequence stabilizes the semiquinone (sq) form, as a result, raising the E_2 value in particular.

Keywords: flavodoxin; FMN; hydrogen bonding; polarity; redox potentials

The redox potential of an electron transfer protein is of prime importance in relation to its function, where the correlation between protein structure and redox potential helps explain how nature has adapted proteins to their specific functions. In the past, this has been studied for a range of flavodoxins, small (14–23 kDa) acidic α/β proteins that contain a single noncovalently bound flavin mononucleotide (FMN) cofactor, from different organisms. In vivo they act as remarkably versatile low potential one-electron donors in a range of reactions (Mayhew and Tollin 1992) in mainly prokaryotic organisms, including obligate and facultative anaerobes, microaerophiles, and photosynthetic cyanobacteria, as well as in both red and green eukaryotic algae. In the photosynthetic bac-

Reprint requests to: Gerard W. Canters, Leiden Institute of Chemistry, P.O. Box 9502, 2300 RA Leiden, The Netherlands; e-mail: canters@chem.leidenuniv.nl; fax: +31-71-527-4349.

Abbreviations: FMN, flavin mononucleotide; RMS, root mean square; ox, oxidized; sq, semiquinone; hq, hydroquinone.

Article and publication are at http://www.proteinscience.org/cgi/doi/10.1110/ps.051582605.

teria *Anabaena*, for example, it replaces ferredoxin as an electron shuttle from photosystem I to ferredoxin-$NADP^+$ reductase under iron-deficient conditions (Sykes and Rogers 1984).

Flavodoxin II from *Azotobacter vinelandii* ATCC 478, the subject of this article, has been implicated in electron transfer to nitrogenase, where its synthesis was coinduced with nitrogenase upon introduction of *A. vinelandii* cells to nitrogen-fixing conditions after growth on NH_4Cl (Klugkist et al. 1986a). This flavodoxin is a so-called "long-chain" flavodoxin and has one of the lowest E_1 midpoint potentials found within the flavodoxin family (Steensma et al. 1996; see below).

Two subgroups have been identified within the flavodoxin family, the short-chain and the long-chain flavodoxins. The long-chain flavodoxins are up to 38 residues longer than the short-chain flavodoxins, mainly due to a long inserted loop of 22 residues in the final strand of the central β-sheet, toward the end of the protein. Flavodoxin II from *A. vinelandii* contains this insertion and is therefore considered to be a member of this subgroup. The distinction between long- and short-chain flavodoxins appears to parallel a difference in redox potentials for these proteins. FMN, both when free in solution and bound to apoflavodoxin, can exist in three redox states, namely oxidized (ox), one-electron reduced semiquinone (sq), and two-electron reduced hydroquinone (hq). For FMN free in solution, the midpoint potential for the ox/sq redox couple, E_2, is lower than that of the sq/hq potential, E_1. However, complex formation with apoflavodoxin alters these potentials dramatically, inducing an inversion as well as a substantial separation between them. As a result, flavodoxin can transfer electrons in two discrete one-electron steps (Lostao et al. 1997).

Three-dimensional structures are known of oxidized flavodoxins from both subgroups, namely, from *Clostridium beijerinckii* (Burnett et al. 1974) and *Desulfovibrio vulgaris* (Watt et al. 1991) for the short-chain and from *Anabaena variabilis* (Rao et al. 1992), *Chondrus crispus* (Fukuyama et al. 1992), *Escherichia coli* (Hoover and Ludwig 1997), *Helicobacter pylori* (Freigang et al. 2002), *Megasphaera elsdenii* (van Mierlo et al. 1990), and *Anacystis nidulans* (Smith et al. 1983) for the long-chain flavodoxins. Additionally, structures of the sq and/or hq forms of the flavodoxins from *A. nidulans*, *C. beijerinckii*, and *D. vulgaris* are also available (Smith et al. 1977; Watt et al. 1991; Ludwig and Luschinsky 1992; Romero et al. 1996; Hoover et al. 1999). The combination of structural data with mutagenesis of identified key residues has resulted in a general picture where it appears that the separation of the midpoint potentials in flavodoxin is effected by the differential stabilization by the apoflavodoxin of the three oxidation states of FMN. In all three structures of flavodoxin semiquinones listed above, a striking difference in the flip of the 58–59 backbone peptide (*A. vinelandii* numbering) upon reduction to the sq form was observed (Watt et al. 1991; Ludwig and Luschinsky 1992). The hydrogen bond then formed between the carbonyl of residue 58 and N5 of the FMN stabilizes the neutral semiquinone in the protein and is purported to be the basis of the positive shift of the ox/sq potential compared with FMN free in solution (Smith et al. 1977; Ludwig et al. 1997; Hoover et al. 1999). The identity of one of the residues within this 58–59 peptide is also known to be a crucial determinant of E_2 (Ludwig et al. 1997; Chang and Swenson 1999). The exceptionally low sq/hq E_1 potentials in flavodoxins, on the other hand, are thought to be brought about by specific destabilizing electrostatic interactions between the anionic hq and the FMN binding site, which contains patches of uncompensated negatively charged residues (Zhou and Swenson 1996a,b). In addition, sandwiching of the FMN between two aromatic residues not only is unfavorable for the charged hq but also actively excludes solvent from the FMN binding pocket, thus maintaining an apolar environment (Swenson and Krey 1994; Lostao et al. 1997; McCarthy et al. 2002).

E_2 in particular appears to be higher in general for the short-chain compared with the long-chain flavodoxins (Fig. 1). The 22-residue insertion that differentiates the long- and short-chain subgroups does not, however, contact the FMN cofactor and, as such, is unlikely to be the source of the differences in potentials, as has previously been noted (Steensma et al. 1998). In fact, a recent study of shortened variants of the long-chain flavodoxin from

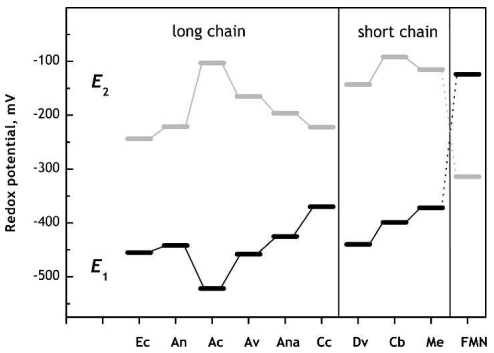

Figure 1. The E_1, sq/hq, and E_2, q/sq, midpoint potentials for long- and short-chain flavodoxins from different sources at pH 7.0, in mV. From *left* to *right*: *E. coli* (Hoover and Ludwig 1997), *A. nidulans* (Hoover et al. 1999), *A. chroococcum* (Deistung and Thorneley 1986), *A. vinelandii* (Steensma et al. 1996), *Anabaena* 7120 (Paulsen et al. 1990), *C. crispus* (Sykes and Rogers 1984), *D. vulgaris* (Curley et al. 1991), *C. beijerinckii* (Mayhew 1971), *M. elsdenii* (Mayhew et al. 1969), and finally, FMN free in solution (Anderson 1983), with E_1 and E_2 inverted with respect to the flavodoxins. For the cases where the potentials were not measured at pH 7.0, a change of −59 mV/pH unit was applied to estimate E_2 (E_1 was assumed to be pH independent above pH 7.0).

Anabaena indicated that the loop was only indirectly responsible for stabilizing the protein complex with FMN and was more likely to be involved in the recognition of partner proteins (Lopez-Llano et al. 2004a,b).

While research has continued into the details of the physiological role of flavodoxins, such as its role in the kinetic regulation of nitrogenase (Duyvis et al. 1998), its ease of expression and purification as well as stability has made it a popular model for a number of more general biochemical studies, in addition to the redox potential studies described above. For flavodoxin II from *A. vinelandii*, these include functional studies of electron transfer to other (nonphysiological) partner proteins (Cheddar et al. 1986; De Francesco et al. 1987), kinetics of flavin binding to apoflavodoxin (Barman and Tollin 1972; Pueyo et al. 1996), and electrochemical studies (Steensma et al. 1996), as well as protein folding and unfolding studies (van Mierlo et al. 2000; Bollen et al. 2004). Despite the wealth of information available on the characteristics and reactivity of this particular flavodoxin, only the secondary structure content of the protein is known from NMR spectroscopic studies (Steensma et al. 1998), as well as a predicted three-dimensional structure obtained by alignment and modeling using the structure of the *A. nidulans* flavodoxin (Drummond 1986).

Here we report the structure of the oxidized form of the Cys69Ala (C69A) mutant of flavodoxin II from *A. vinelandii* as solved by X-ray diffraction to a resolution of 2.25 Å using molecular replacement. While the basic fold of the flavodoxin resembles that of other known flavodoxins, several unique features stand out. An eight-residue loop purported by analogy to be involved in partner protein complex formation is identified at the surface of the protein. Focusing on the local structure around the FMN binding pocket, a striking difference was noted in the absence of a hydrogen bond to the N5 of FMN, contrary to all other structures of oxidized long-chain flavodoxins known. The presence of a leucine instead of a conserved tryptophan on the *re* face of the FMN results in a more polar FMN binding site, while a significantly larger cluster of negatively charged residues is found around the N1 of the FMN than in other flavodoxins. Both these factors are known determinants of E_1, the sq/hq potential. Despite the fact that only the E_1 redox couple is biologically relevant, close study of the structure of flavodoxins in the various redox states has been instrumental in furthering understanding of how variations in composition and structure modulate both E_1 and E_2 redox potentials of this protein family in particular, with implications for redox proteins in general. In this *A. vinelandii* flavodoxin, the structure suggests destabilization of the ox and hq forms of the protein, while stabilization of the sq form moves the ox/sq E_2 redox potential to a relatively high value. The discussion affords new insights into how variations in protein composition and structure can modulate their redox potentials.

Results and Discussion

The crystal structure determination of A. vinelandii *C69A flavodoxin II*

The crystal structure of *A. vinelandii* C69A flavodoxin II was solved at 2.25 Å resolution using molecular replacement with a homology model based on the *Anabaena* flavodoxin structure (Rao et al. 1992; Burkhart 1995). The protein crystallized with two monomeric molecules in the asymmetric unit, called A and B, which are related by a 133° rotation. The refinement statistics and contents of the final model are given in Table 1. Except for some solvent-exposed side chains, the molecules are clearly defined in density. Superposition of the Cα atoms of the two molecules gives a root mean square (RMS) difference of 0.7 Å. Excluding residues that differ by more than 3 σ (residues 1, 59, 178, and 179), the RMS difference decreases to 0.38 Å. Taking into account only the nonglycine and nonproline residues and discounting the first and last residues of each molecule, 268 residues (88.2%) are in the most favored region of the Ramachandran plot, 36 residues (11.8%) are in the additional allowed regions, and none of the residues are in the generously allowed regions or in the disallowed regions.

Table 1. *Data collection, refinement, and model statistics*

Data collection			
Resolution (Å)	30–2.25		
Total observations	156,381		
Unique observations	17,468		
Completeness (%)	92.0		
Completeness last shell (2.33–2.25 Å) (%)	85.4		
R_{merge} (%)	7.2		
R_{merge} last shell (2.33–2.25 Å) (%)	49.2		
I/σ	16.1		
I/ σ last shell (2.33–2.25 Å)	2.4		
Refinement statistics			
R-factor (%)	22.2		
Free R-factor (%)	27.9		
RMS deviation from ideality			
Bond lengths (Å)	0.0068		
Bond angles (°)	1.32		
Model statistics			
Polypeptide chain	A	B	Total
No. of amino acid residues	179	179	358
No. of FMN groups	1	1	2
No. of water molecules			221
No. of sulphate ions			6

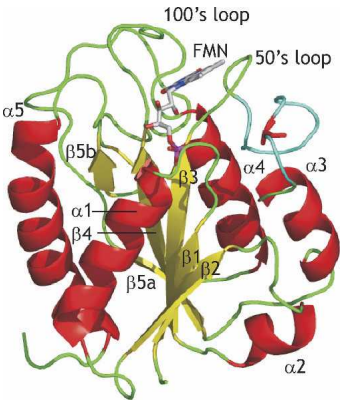

Figure 2. The three-dimensional fold of *A. vinelandii* flavodoxin II, with α-helices shown in red; β-sheets, in yellow; and random coil, in green. The inserted loop of residues 61–71 is colored cyan, and the mutation Cys69Ala is shown in red sticks in the *middle* of that loop. The FMN cofactor is also represented in stick form at the *top* of the protein.

The polypeptide fold of A. vinelandii *C69A flavodoxin II*

C69A flavodoxin II from *A. vinelandii* is the longest flavodoxin to date for which a structure has been determined. Its three-dimensional fold is shown in Figure 2 and consists of the α/β fold common to all flavodoxin structures presently known. The main secondary structure elements of the protein were defined from the Protein Data Bank (PDB) coordinates using the DSSP program by Kabsch and Sander (1983). The central core of the protein is made up of a highly conserved five-stranded parallel β-sheet, the final strand of which is interrupted by a 22-amino-acid insertion between β_{5a} and β_{5b}, characteristic of long-chain flavodoxins. There is, however, more variability between different flavodoxins in the number and length of the α-helices that pack against the central β-sheet core. Here, a total of five α-helices were identified, with helices 1 and 5 found together on one face of the sheet, while helices 2, 3, and 4 are clustered on the other face. A short helical region of 1.5 turns, α_2, was found after a 3_{10} helix in between strands β_2 and β_3.

Structural comparisons to other flavodoxins

The α-carbon backbone of molecule A of the *A. vinelandii* flavodoxin was superposed onto all other known structures of long-chain flavodoxins, and the RMS difference was calculated for each pair of proteins (Table 2). The structures of flavodoxins from five other sources superpose well onto the *A. vinelandii* flavodoxin, with RMS differences < 1 Å for all structures, except for that from *C. crispus*, the only eukaryotic flavodoxin in the group. Interestingly, flavodoxin from *A. vinelandii* appears to resemble that from *H. pylori* most closely in structure, with an RMS difference of 0.89 Å, while the amino acid sequence identity between the two proteins of 39% is comparatively low. The two structures only deviate significantly at the points where the longer *A. vinelandii* contains insertions, namely, in turns Lys23–Thr29, which connects α_1 and β_2, and Asp119–Gly121, which connects α_4 and β_5. Similarly a single residue insertion in the *H. pylori* flavodoxin of Gly69 leads to a slightly different position of the Gly83–Ser87 loop in the *A. vinelandii* flavodoxin. The stretch between strands β_2 and β_3 typically shows more diversity in fold between the various flavodoxins. Although the flavodoxin from *A. vinelandii* is most identical to that from *Anabaena*, the former has a 3_{10} helix followed by a short α-helix at this point, while the latter does not exhibit any helical structure in this region. The flavodoxins from *A. nidulans* and *C. crispus* have a 3_{10} helix and a short single-turn α-helix here, respectively. Additionally, α_3 of *A. vinelandii* is relatively long, more similar to the flavodoxin from *Anabaena* than to those from *A. nidulans* or *C. crispus*.

Structure-based alignment of the flavodoxin sequences in Figure 3 also reveals that, compared with other long-chain flavodoxins, the *A. vinelandii* flavodoxin has an additional inserted loop of residues 64–71. These eight amino acids map onto a stretch following

Table 2. *RMS differences in angstrom between superpositions of the α-carbon atoms of all long-chain flavodoxin structures*

	A. vinelandii	*H. pylori*	*E. coli*	*A. nidulans*	*Anabaena 7120*
A. vinelandii	—	—	—	—	—
H. pylori	0.89 (39%)	—	—	—	—
E. coli	0.93 (44%)	0.83 (43%)	—	—	—
A. nidulans	0.97 (41%)	0.96 (38%)	0.83 (45%)	—	—
Anabaena 7120	0.99 (47%)	0.95 (42%)	0.84 (46%)	0.54 (70%)	—
C. crispus	1.17 (39%)	1.22 (34%)	1.25 (37%)	1.14 (36%)	1.20 (41%)

The amino acid sequences were compared using the local alignment program BLAST, and the identity between them is indicated in parentheses.

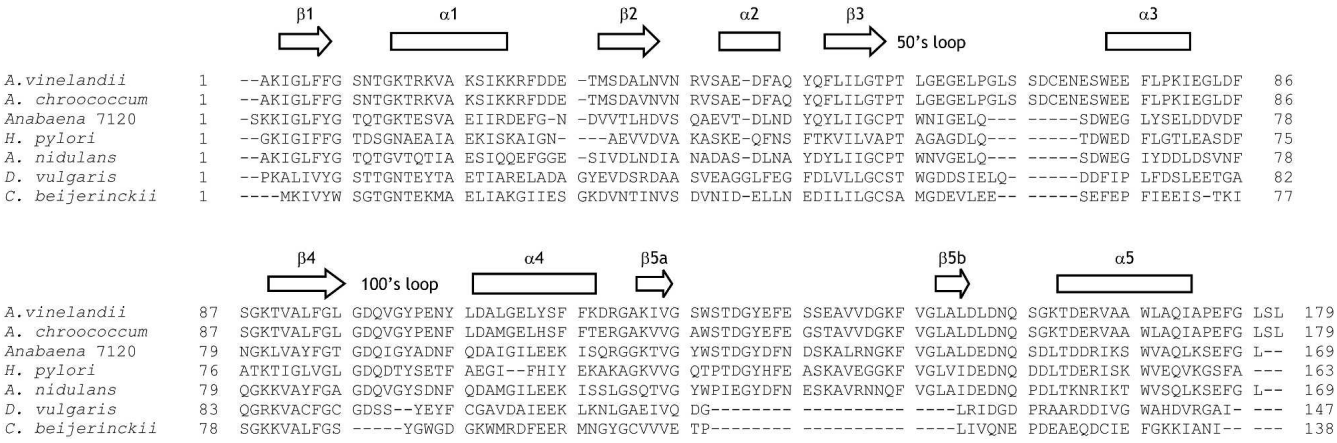

Figure 3. Structure-based sequence alignment using SEQUOIA v0.9.7 (Bruns et al. 1999) of the oxidized long-chain flavodoxins from *A. vinelandii*, *Anabaena* 7120 (PDB entry 1RCF; Burkhart 1995), *H. pylori* (PDB entry 1FUE; Freigang et al. 2002), and *A. nidulans* (PDB entry 1CZU; Drennan et al. 1999) and the oxidized short-chain flavodoxins from *D. vulgaris* (PDB entry 1J8Q; Artali et al. 2002) and *C. beijerinckii* (PDB entry 5NLL; Ludwig et al. 1997). The 22-residue loop that differentiates short- and long-chain flavodoxins is clearly visible inserted between strands β_{5a} and β_{5b}. The primary sequence of *A. chroococcum* flavodoxin was aligned with that of *A. vinelandii* using CLUSTALW version 1.81 (Thompson et al. 1994). The main secondary structure elements of the *A. vinelandii* protein were defined from the PDB coordinates using the DSSP program (Kabsch and Sander 1983) and are indicated *above* the amino acid sequence alignment.

strand β_3, colored cyan in Figure 2, at the FMN binding end of the protein. The insertion takes on the conformation of a short 3_{10} helix, followed by a turn and a loop that precede the start of α_3. An analogous loop has previously also been identified by sequence analysis in the 94% identical *A. chroococcum* flavodoxin (Peelen et al. 1996), the three-dimensional structure of which has never been released (Thorneley et al. 1994). However, from two-dimensional NMR data, the loop was inferred to be at the protein surface and was shown to be involved in complex formation with the Fe protein of nitrogenase (Peelen et al. 1996). Our structure of the *A. vinelandii* flavodoxin corroborates the former result, clearly showing this loop to be solvent-exposed.

The protein used for this study is the Cys69Ala (C69A) mutant, which has widely been used for functional studies, as it does not dimerize via the cysteine thiol group like wild type does (Yoch 1975), while retaining the redox properties of the wild-type protein (Steensma et al. 1996). The Cys69Ala mutation sits in the middle of the above loop on the surface, toward one side of the protein with no direct contacts with the FMN cofactor (Fig. 2). This is consistent with the unchanged redox potentials of this mutant. Additionally, as the Cβ carbon of Ala69 is solvent-exposed, assuming that the mutation does not cause conformational changes, by analogy the thiol group of the cysteine residue in the wild-type protein may also be expected to be solvent-accessible. This may explain the tendency of the wild-type protein to dimerize over time (Yoch 1975).

A single phosphate group is present in the structure as part of the FMN cofactor. The gene for flavodoxin II used for this study is identical to that cloned from *A. vinelandii* strain OP Berkeley (Bennett et al. 1988), that has also been expressed heterologously in *E. coli* (Taylor et al. 1990). This crystal structure confirms an earlier notion that this flavodoxin form does not contain a covalently bound phosphate (Klugkist et al. 1986b), as was also found for the recombinant flavodoxin from *A. vinelandii* strain OP Berkeley (Taylor et al. 1990).

A total of seven solvent molecules were found buried in the interior of the protein, occupying comparable positions in both molecules in the asymmetric unit. The positions of these water molecules with respect to the three-dimensional fold of the flavodoxin molecule are illustrated in Figure 4A. Two of them, colored green, were found to interact with residues at the top ends of strands β_3 and β_4, and β_4 and β_5. Two others, colored light blue, bridge the loop connecting the end of α_2 to the start of β_3, and to the ^{152}D-L-D-N^{155} loop between the end of β_5 and the start of α_5, respectively. A structurally conserved solvent molecule was also found between Leu93 on β_4 and the end of β_{5a}, just at the start of the inserted loop common to long-chain flavodoxins; it is visible as the dark sphere toward the back of the molecule in Figure 4A. Finally, two more water molecules, colored red, were identified in the cavity adjacent to the more buried *re* face of the FMN. These latter two will be discussed in more detail later in the article. However, all mentioned solvent molecules appear to play a structural role in the packing of the protein. This is confirmed by the fact that they mostly occupy positions similar to those of water molecules found in other long-chain flavodoxins (Burkhart 1995; Hoover and Ludwig 1997; Drennan et al. 1999).

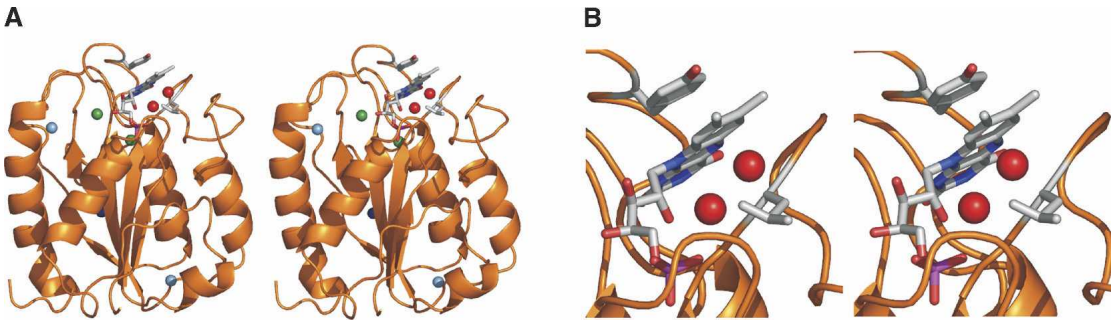

Figure 4. (*A*) Stereo views showing the positions of the structured solvent molecules, represented as spheres, with respect to the whole flavodoxin molecule, where the two light blue waters bridge α-helices and β-strands while the two green waters bridge the ends of two β-strands. A single black water molecule is found toward the *back* of the flavodoxin, at the start of the 22-residue insertion in β5 strand of the sheet. (*B*) Zoom in on the FMN binding site flanked by Tyr102 and Leu57 at the *top* of the molecule in *A* where two red waters can be seen to lead from the cavity on the *re* face of the FMN created by the smaller leucine 57 side chain to the surface of the protein.

The FMN binding pocket

As with other flavodoxins, the FMN cofactor binds noncovalently at one end of the central β-sheet, with the pyrimidine part of the molecule buried in the interior of the protein, and with the dimethyl benzene edge that has been proposed to mediate electron transfer, solvent exposed (Mayhew and Ludwig 1975). The FMN molecule is bound in a very flat conformation compared with other flavodoxins. Superposition of the α-carbon atoms of different flavodoxins as described above shows that the FMN sits at a very similar angle with respect to the protein fold, except for the three flavodoxins that have a nontryptophan substitution at position 57 (*A. vinelandii* numbering). The FMN in these proteins is more tilted. For example, the FMN in the *C. beijerinckii* flavodoxin is tilted by some 25° compared with that from *Anabaena*. This angle is closer to 15° in both *H. pylori* and *A. vinelandii*. The isoalloxazine ring in both these flavodoxins is also completely planar, as opposed to a slight butterfly-like bend that has been observed for other flavodoxins, which is ~8° for the *Anabaena* flavodoxin.

The different parts of the FMN cofactor associate with the flavodoxin polypeptide chain through a variety of interactions, including hydrogen bonds and hydrophobic stacking. Three main regions of apoflavodoxin implicated in the noncovalent binding of FMN in other flavodoxins are also closely associated with the flavin in *A. vinelandii* flavodoxin, as detailed below.

First, the extended phosphorbityl side chain acts to anchor the cofactor to the protein via an extensive network of hydrogen bonds, as summarized in Table 3 and shown in Figure 5A. The hydroxyl groups of the ribityl chain as well as the phosphate oxygen atoms form hydrogen bonds mainly to backbone amide and carbonyl groups of the protein and to two solvent molecules. In particular, numerous interactions are present between the phosphate oxygen atoms and backbone amides as well as side-chain hydroxyl groups of the ^{9}S-N-T-G-K-T^{14} loop, as deduced from the H-bonding distances between the atoms. This loop, cru-

Table 3. *Hydrogen bond interactions between FMN and apoflavodoxin or water atoms in* A. vinelandii *flavodoxin II for molecule A*

FMN atom	Protein/water atom	Distance (Å)
N1	O 56 Thr	3.52
	N 98 Asp	3.00
O2	N 98 Asp	3.37
	O 105 Asn	3.29
	N 107 Leu	2.78
N3	O 105 Asn	2.71
O4	N 60 Gly	3.32
	W22	2.64
N5	W22	3.17
O2*	O 56 Thr	2.68
	N 56 Thr	3.27
O3*	NZ 13 Lys	3.67
	OD1 154 Asp	2.62
O4*	W2	2.90
OP1	OG 9 Ser	2.57
	N 13 Lys	3.54
	N 14 Thr	2.86
	OG1 14 Thr	2.63
OP2	N 10 Asn	2.95
	N 11 Thr	3.06
	OG1 11 Thr	3.32
	W 28	2.56
OP3	N 11 Thr	3.38
	OG1 11 Thr	2.45
	N 12 Gly	3.12

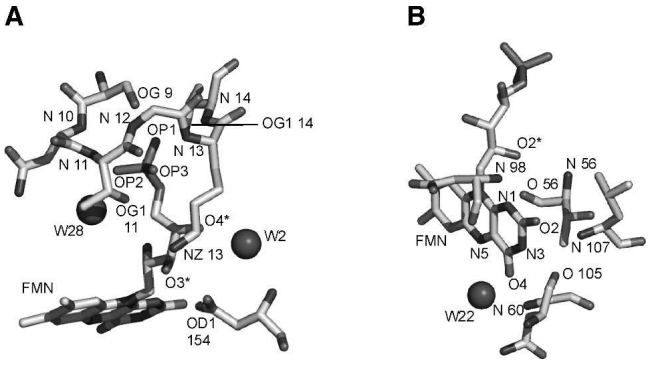

Figure 5. The FMN binding site in oxidized *A. vinelandii* flavodoxin II showing the hydrogen bonding partners from both main-chain and side-chain atoms (denoted by atom name, followed by the residue number) of the flavodoxin as well as waters (denoted W) to the phosphoribityl side chain of the FMN (including the phosphate-binding loop consisting of residues 9–14 including the crucial Gly12) (*A*) and the isoalloxazine part of the FMN (*B*).

cially requiring Gly at position 12, has been identified as a consensus sequence for phosphate binding in flavodoxins (Ludwig and Luschinsky 1992). It has a conformation very similar to that observed in other flavodoxins.

Second, the so-called 50s loop following β_3 identified in other flavodoxins is also closely involved in FMN binding in the *A. vinelandii* flavodoxin, in particular residues ^{56}T-L-G-E-G^{60}. Despite considerable variation in sequence in this region between species, the conformation and interaction of these residues with respect to the FMN is conserved. Figure 6 shows how this four-residue loop adopts almost identical positions in *Anabaena*, *C. beijerinckii*, and *A. vinelandii*, with many backbone carbonyl and amide groups within hydrogen bonding distance of the FMN. Unique to the *A. vinelandii* flavodoxin is an interaction between Thr56 and N1 of FMN as well as O2* of the ribityl side chain (Table 3; Fig. 5B). The two-residue peptide that undergoes a backbone flip upon reduction of the ox to the sq and hq forms is the 58–59 peptide also located in this loop. In all structures of oxidized flavodoxins, the backbone carbonyl of residue 58 points away from the N5 atom of FMN in an "O-down" conformation, whereas in the semiquinone state, determined for the flavodoxins from *C. beijerinckii*, *D. vulgaris*, and *A. nidulans*, the carbonyl group assumes an "O-up" conformation and points to the N5 (Watt et al. 1991; Ludwig and Luschinsky 1992; Hoover et al. 1999). Our structure shows that in *A. vinelandii* flavodoxin in the oxidized state, the carbonyl group of Gly58 is also in the O-down conformation and points away from the N5, toward the *re* face of the FMN cofactor (Fig. 6C). This is similar to the carbonyl groups of the analogous residues in the long-chain *Anabaena* and the short-chain *C. beijerinckii* flavodoxins (Fig. 6A,B, respectively).

Finally, numerous hydrogen-bonding interactions between FMN and the apoprotein were identified in the 100s loop, from residues 98–107. A number of backbone amide and carbonyl groups are present within hydrogen bonding distance of the isoalloxazine ring of FMN, in particular from residues 98, 105, and 107 to N1, O2, and N3 of FMN (Table 3). Figure 5B shows the main hydrogen bonding partners of the flavodoxin polypeptide to the isoalloxazine part of the FMN, both from the 50s and 100s loop. The 100s loop also contains Tyr102, which flanks the FMN cofactor shielding its *si* face from the solvent and which has been shown to play

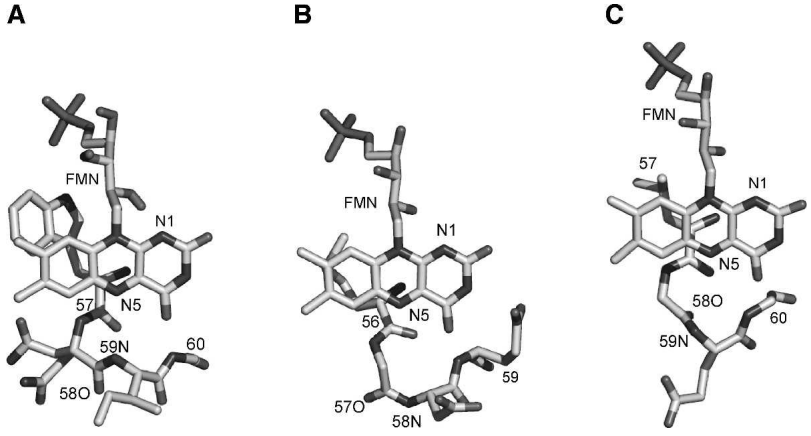

Figure 6. Conformation of the four-residue turn in the 50s loop that contacts the FMN, in the same orientation from *Anabaena* (*A*), *C. beijerinckii* (*B*), and *A. vinelandii* (*C*) flavodoxin. The residue numbers are shown *next to* the backbone amides of the corresponding amino acids, where the backbone amide of residue 59 in *A* can clearly be seen to point toward the N5 of FMN, while in *B* and *C* the corresponding amide groups of residues 58 and 59, respectively, have geometries that are unsuitable for hydrogen bonding to the N5.

an important role in the energetics of FMN binding through coplanar aromatic stacking interactions (Zhou and Swenson 1996b; Lostao et al. 2000).

Distinctive features of FMN binding in A. vinelandii *flavodoxin and consequences for its midpoint potentials*

H-bonding to N5 of FMN destabilizes the ox form

The hydrogen bonding state of the N5 of FMN in the oxidized flavodoxin is also known to affect the E_2 redox potential by stabilizing the oxidized form of the protein (Rao et al. 1992; Hoover et al. 1999). In all structures of oxidized long-chain flavodoxins known to date, a hydrogen bond is found from a residue within the 50s loop to the unprotonated FMN N5. In *Anabaena* (Fig. 6A), *A. nidulans*, and *E. coli*, the donor is the backbone amide of residue 59, while in *C. crispus* it is the side-chain hydroxyl group of the adjacent Thr58. Although these hydrogen-bond donors are at between 3.1 Å and 3.6 Å from N5 in the different flavodoxins, their geometry is favorable, pointing directly toward the N5 (Burkhart 1995; Hoover and Ludwig 1997; Drennan et al. 1999). Additionally, the apolar environment of the FMN binding site may increase the strength of the interaction (Rao et al. 1992), and more compellingly, direct NMR evidence for hydrogen bonding to N5 exists (Stockman et al. 1988; Chang and Swenson 1999). Although the hydrogen bond is broken upon reduction of the flavodoxin to the semiquinone, N5 subsequently makes a hydrogen bond with the carbonyl oxygen atom as described above, which requires the backbone peptide plane to flip (see above). However, in the oxidized *A. vinelandii* flavodoxin, no candidate for a hydrogen-bonding interaction with N5 could be found (Fig. 6C). The closest backbone amide group is that of Glu59, at a distance of 4.0 Å from N5, but it is in an unfavorable position for hydrogen bonding. In this sense, the oxidized *A. vinelandii* protein resembles the short-chain flavodoxins from *D. vulgaris* (Romero et al. 1996) and *C. beijerinckii* (Fig. 6B) (Chang and Swenson 1999) more closely, where no potential hydrogen bond donor is near the N5 atom either. It is likely that the absence of a hydrogen bond to N5 in the oxidized form of the protein destabilizes the ox form of the FMN, making reduction comparatively easier and yielding a higher E_2 value.

Gly58 stabilizes the sq form

From sequence alignments, the residue at position 58 is most commonly a glycine in short-chain and an asparagine in long-chain flavodoxins. Uncommonly for a long-chain flavodoxin, the one from *A. vinelandii* has a glycine at this position. While the glycine can optimally accommodate the O-up conformation at that position of the type II′ turn found in flavodoxin semiquinones (Hutchinson and Thornton 1994), the Cβ of the asparagine found in the long-chain *A. nidulans* flavodoxin makes very close contact with the following amide group, raising the energy of the O-up conformation (Hoover et al. 1999). That this residue affects the stabilization of the semiquinone bound to flavodoxin and thus the redox potentials was confirmed by the Asn58Gly mutant of the long-chain *A. nidulans* flavodoxin, which had an ox/sq potential 46 mV more positive than that of the wild type, while its sq/hq potential was lowered by 26 mV (Hoover et al. 1999). On the other hand, mutants of the short-chain *C. beijerinckii* flavodoxin where the homologous Gly57 residue was replaced by alanine, asparagine, aspartate, and proline all had ox/sq potentials that were reduced by ~60 mV, while the Gly57Thr mutant with its bulkier β-branched side chain had an E_2 that was even lower, by 180 mV (Ludwig et al. 1997). Direct measurement of the strength of the N5H···O57 hydrogen bond in this series of mutants by NMR definitively proved this effect, with a strong correlation between the temperature coefficients of the N5H and both E_2 and binding energy of the FMN semiquinone to the flavodoxin (Chang and Swenson 1999). Thus it is conceivable that the atypical glycine at this position in the flavodoxin from *A. vinelandii* may be a factor in shifting the ox/sq potential to a more positive value. The analogous residue in the *H. pylori* flavodoxin is also a glycine; however, its redox potentials are not known. The long-chain flavodoxin from *E. coli* may provide further support for the proposed correlation between E_2 and the nature of the residue at position 58: The ox/sq potential for this flavodoxin is among the lowest of all those known, where the protein has a bulky tyrosine residue here (Hoover and Ludwig 1997).

Additional charges close to the N1 of FMN further destabilize the hq form

Up to 11 acidic amino acids were found within 15 Å of N1 of FMN in the *A. vinelandii* flavodoxin, namely, the aspartates 68, 98, 108, 152, and 154 and the glutamates 59, 61, 104, 134, 136, and 139. Several of these residues are situated in the 100s loop, including the closest charged group at a distance of 3.0 Å, the carboxylic moiety of Asp98. Conversely, only three basic residues are present, and then only at the very periphery of the 15 Å radius from the FMN N1, with the positively charged side chains solvent-exposed at the surface of the protein instead of pointing toward the FMN binding pocket. This acidic character of the binding pocket around the N1 is known to be a major determinant of the sq/hq potential E_1. The FMN hydroquinone in flavodoxins from both *M. elsdenii* (Franken et al. 1984)

and *D. vulgaris* (Vervoort et al. 1986) have been found to exist as anions, while evidence for sterical hindrance preventing protonation at N1 was found for the *C. beijerinckii* flavodoxin (Ludwig et al. 1990). The negative charges of the side chains destabilize the anionic hydroquinone, creating an unfavorable electrostatic environment that makes the reduction of the semiquinone more difficult. A patch of uncompensated negatively charged residues is commonly found grouped around the N1 of FMN in flavodoxins, and totals six to seven residues in both the *D. vulgaris* (Zhou and Swenson 1996b) and *A. nidulans* (Hoover et al. 1999) flavodoxins. Zhou and Swenson (1995) systematically mutated all six acidic residues in the *D. vulgaris* flavodoxin, with the effect that E_1 was raised by ~15 mV on average per neutralized amino acid. If by analogy the hq of the *A. vinelandii* flavodoxin is also negatively charged (Stockman et al. 1988), by this gauge, the five additional negative charges observed in this protein could potentially result in a negative shift in E_1 in the order of 75 mV.

Leu at the re *face of FMN results in a more polar FMN binding site and stabilizes the hq form*

While in most flavodoxins the FMN is stacked against a tyrosine on its *si*, or outer, face, more variability has been found in the amino acid present on its *re*, or inner, face. This is most commonly a tryptophan; however, nonaromatic residues have also been found. In *A. vinelandii* flavodoxin, a leucine residue is present. As a result, an open cavity is created at the *re* face of the cofactor, making it much more accessible to solvent. In fact, in both molecules of the asymmetric unit, two water molecules with low B-factors occupy this cavity in identical positions. They connect the innermost ring of the FMN to the surface of the flavodoxin (Fig. 4B). The FMN in the *A. vinelandii* flavodoxin is the most solvent-exposed one in the long-chain flavodoxins of known structure, where values as calculated by NACCESS (S.J. Hubbard and J.M. Thornton, University College London) for the surface accessibility for FMN in the five long-chain flavodoxins of known structure and potentials are as follows: *A. vinelandii* (averaged for molecule A and B), 114.8 Å; *Anabaena*, 93.9 Å; *A. nidulans*, 100.1 Å; *C. crispus*, 98.7 Å; and *E. coli*, 99.7 Å. The presence of smaller and/or polar residues stabilizes the anionic FMN hq in the protein, thus shifting the sq/hq potential to more positive levels. This was corroborated by the mutation of the analogous Trp60 in the *D. vulgaris* flavodoxin to alanine, which raised E_1 by 83 mV (Mayhew et al. 1996), while the Trp57Leu *Anabaena* flavodoxin mutant had an E_1 that was higher by 30 mV (Lostao et al. 1997). A methionine flanks the *re* face of the *C. beijerinckii* flavodoxin FMN, and a similar FMN-to-surface water channel is present. This flavodoxin has one of the highest E_1 potentials known (Ludwig et al. 1990). Intriguingly, however, despite the small leucine residue and the presence of two water molecules within close proximity of the FMN, at −458 mV (Steensma et al. 1996) the *A. vinelandii* flavodoxin appears to have one of the lowest E_1 values of all flavodoxins (Fig. 1). It is possible that the additional negative charges clustered around the N1 compensate for the increased polarity of the FMN binding site in this protein.

Comparisons between the two Azotobacter *flavodoxins*

The *A. chroococcum* flavodoxin has a sq/hq potential, which, at −522 mV, is even more negative than that of the *A. vinelandii* flavodoxin. Aligning the two protein sequences shows that the *A. chroococcum* flavodoxin also contains the additional negatively charged residues, as well as a phenylalanine instead of a tyrosine at position 106 (Fig. 3). In the *A. vinelandii* structure, this residue was found within 5 Å of the most buried ring of the FMN, in an almost coplanar conformation. No other differences could be mapped to locations close to the FMN that could account for the extremely low E_1 of the *A. chroococcum* flavodoxin, which reinforces the overriding influence of the acidic nature of the FMN binding site.

We report here the first crystal structure of flavodoxin II from *A. vinelandii*, of the monomeric C69A mutant. In general, the structure closely resembles that of other long-chain flavodoxins, with the exception of an eight-residue insertion between β_3 and α_3, which is found as a short 3_{10} helix followed by a turn at the surface of the protein. The C69A mutation is solvent-exposed, as was previously proposed due to the propensity of the wild-type protein to form disulphide-bridged dimers.

On the whole, the interactions between the FMN cofactor and the apoflavodoxin are similar to those previously identified in other long- and short-chain flavodoxins, although variations in the amino acid sequence have resulted in several novel hydrogen bonds. More noteworthy, however, is the absence of a hydrogen bond to the N5 atom of the isoalloxazine ring, observed in all structures of oxidized long-chain flavodoxins determined to date. This is expected to destabilize the oxidized FMN and may in part explain the relatively high ox/sq E_2 potential of this flavodoxin. In addition, a glycine is present in the two-residue peptide that flips upon reduction of the protein, instead of the asparagine typical of long-chain flavodoxins. In both these characteristics, the *A. vinelandii* flavodoxin resembles the short-chain flavodoxins from *C. beijerinckii* and *D. vulgaris* more closely, where this is mirrored in their comparable E_2 values.

A cavity is found on the *re* face of the FMN, due to a leucine residue flanking the cofactor instead of the more common tryptophan. A short channel consisting of two water molecules leads from this cavity to the surface of the protein. As a result, the FMN in this flavodoxin is much more solvent-exposed, an effect which is known to stabilize the anionic hq form and raise the sq/hq E_1 potential. On the other hand, destabilization of the hq form is promoted by an exceptionally large cluster of 11 uncompensated negatively charged residues around the anionic FMN N1 atom, almost twice the number found in both short- and long-chain flavodoxins. The more polar FMN binding site counteracts the destabilization of the hq, and the net effect leads to the E_1 value of −458 mV observed. However, differential stabilization of the sq form by the formation of a hydrogen bond to the N5 effectively raises E_2 to a value closer to that of short-chain flavodoxins.

In summary, this structure of the oxidized flavodoxin II of *A. vinelandii* is an important starting point for a deeper understanding of the factors that modulate the redox potential of flavodoxins in general, and this protein in particular. Comparing this structure with other long- and short-chain flavodoxins has allowed us to identify particular features (a more polar FMN binding site due to the Leu–Trp replacement, a large cluster of acidic residues close to the N1) and residues (Gly58 that does not hydrogen bond to N5 in the oxidized state) that may be key to fine-tuning the E_1 and E_2 potentials. Further mutational, biochemical, and structural studies involving these residues will be required to correlate the observed structural and functional differences. Modulations by the interactions of these residues with the FMN result in what may more usefully be considered as a continuous range of E_1 and E_2 values for the different flavodoxins, as opposed to stricter definitions of class and redox potential based on chain length. Finally, NMR techniques can identify residues important for complex formation between flavodoxin and its redox partners. Mapping these onto the three-dimensional structure of the protein may give new insights not only into the nature of the complex but also into the particular pathways that may be involved in the electron transfer reaction.

Materials and methods

Expression and purification of recombinant A. vinelandii *flavodoxin II*

C69A flavodoxin II from *A. vinelandii* ATCC 478 was expressed heterologously in *E. coli* strain TG2 from a pUC19 plasmid containing the mutated Cys69Ala flavodoxin gene (van Mierlo et al. 1998). The large-scale culture was induced with 1 mM IPTG upon inoculation and grown for 24 h before harvesting. The protein was purified according to described protocols and was considered to be pure when the absorption peaks showed a ratio A_{274}/A_{452} of 4.7 (Tollin and Edmondson 1980). The molar absorption coefficient at 452 nm of 11.3 mM^{-1} cm^{-1} (Klugkist et al. 1986b) was used to determine the concentration of flavodoxin.

Crystallization and X-ray data collection

Crystals were grown at room temperature using the sitting drop vapor diffusion method. The reservoir contained 2.8 M ammonium sulphate and 0.1 M Tris buffer (pH 7.0). The drops were made by mixing 2 μL of protein solution (15 mg/mL in 0.1 M Tris buffer [pH 8.0]) and 2 μL of the reservoir solution. Plates and clusters of plate-like crystals grew over a period of between 1 and 2 wk. The crystal used for data collection was transferred to a 4:1 solution of reservoir solution and water. The crystal was subsequently dipped in Al's oil (1:1 paraffin oil and silicon oil) and flash frozen in a stream of evaporating nitrogen gas of 100 K. The crystal belongs to space group $P2_12_12_1$ with cell dimensions $a = 39.01$ Å, $b = 70.54$ Å, and $c = 132.64$ Å. It diffracted to 2.25 Å resolution. Data were collected in house with a MAR CCD detector with CuKα X-rays from a NONIUS FR591 rotating anode generator (Table 1). Data were processed with DENZO and SCALEPACK (Otwinowski and Minor 1997). Reduction to structure factor amplitudes was performed with TRUNCATE (French 1978).

Model building and crystallographic refinement

The structure of flavodoxin II C69A was solved by molecular replacement. The search model was based on the structure of the 47% sequence identical *Anabaena* flavodoxin (PDB code 1RCF; Burkhart 1995) using the 3D-PSSM server (Kelley et al. 2000). This resulted in a model in which the side chains had been modeled by placement with a rotamer library (Bower et al. 1997). Two molecules were located in the asymmetric unit using the molecular replacement program EPMR (Kissinger et al. 1999), yielding a solvent content of 50%. Using data between 10 Å and 4 Å resolution, the correlation coefficient and R-factor of EPMR became 0.227 and 57.0% for the first molecule only and improved to 0.387 and 50.4% when both molecules in the asymmetric unit were included. The two molecules were rigid body refined with CNS (Brunger et al. 1998), resulting in an R-factor of 48% (10–3Å). After a first round of simulated annealing (30–2.25Å, R-factor 37.0%, R-free 42.7%), the electron density map was clear and showed the FMN group that had been omitted from the molecular replacement model. Side chains pointing in the wrong direction and main-chain at insertion points were manually rebuilt using the programs O (Jones et al. 1991) and QUANTA (Accelrys). The improved model was further refined with REFMAC5 (Murshudov 1997). No NCS constraints were used. Water molecules were added, and electron density for six sulphate ions was also present. The final R-factor is 22.3%; the free R-factor, 27.8%. The refinement statistics and information about the final model are listed in Table 1. The geometry of the final model was analyzed using PROCHECK (Laskowski et al. 1993). Figures were prepared using PyMOL (http://pymol.sourceforge.net). The coordinates have been deposited in the PDB (Berman et al. 2000) under accession number 1YOB.

Calculation of surface accessibility of FMN in flavodoxins

The program NACCESS (S.J. Hubbard and J.M. Thornton, University College London) was used to calculate the surface accessibility of the FMN cofactor in $Å^2$ for a number of both long- and short-chain flavodoxins, using the PDB files of each of the proteins as input and the default probe size of 1.4 Å.

References

Anderson, R.F. 1983. Energetics of the one-electron reduction steps of riboflavin, FMN and FAD to their fully reduced forms. *Biochim. Biophys. Acta* **722:** 158–162.

Artali, R., Bombieri, G., Meneghetti, F., Gilardi, G., Sadeghi, S.J., Cavazzini, D., and Rossi, G.L. 2002. Comparison of the refined crystal structures of wild-type (1.34 Å) flavodoxin from *Desulfovibrio vulgaris* and the S35C mutant (1.44 Å) at 100 K. *Acta Crystallogr. D. Biol. Crystallogr.* **58:** 1787–1792.

Barman, B.G. and Tollin, G. 1972. Flavine-protein interactions in flavoenzymes: Thermodynamics and kinetics of reduction of *Azotobacter* flavodoxin. *Biochemistry* **11:** 4755–4759.

Bennett, L.T., Jacobson, M.R., and Dean, D.R. 1988. Isolation, sequencing, and mutagenesis of the nifF gene encoding flavodoxin from *Azotobacter vinelandii*. *J. Biol. Chem.* **263:** 1364–1369.

Berman, H.M., Westbrook, J., Feng, Z., Gilliland, G., Bhat, T.N., Weissig, H., Shindyalov, I.N., and Bourne, P.E. 2000. The Protein Data Bank. *Nucleic Acids Res.* **28:** 235–242.

Bollen, Y.J., Sanchez, I.E., and van Mierlo, C.P. 2004. Formation of on- and off-pathway intermediates in the folding kinetics of *Azotobacter vinelandii* apoflavodoxin. *Biochemistry* **43:** 10475–10489.

Bower, M.J., Cohen, F.E., and Dunbrack Jr., R.L. 1997. Prediction of protein side-chain rotamers from a backbone-dependent rotamer library: A new homology modeling tool. *J. Mol. Biol.* **267:** 1268–1282.

Brunger, A.T., Adams, P.D., Clore, G.M., DeLano, W.L., Gros, P., Grosse-Kunstleve, R.W., Jiang, J.S., Kuszewski, J., Nilges, M., Pannu, N.S., et al. 1998. Crystallography & NMR system: A new software suite for macromolecular structure determination. *Acta Crystallogr. D. Biol. Crystallogr.* **54:** 905–921.

Bruns, C.M., Hubatsch, I., Ridderstrom, M., Mannervik, B., and Tainer, J.A. 1999. Human glutathione transferase A4–4 crystal structures and mutagenesis reveal the basis of high catalytic efficiency with toxic lipid peroxidation products. *J. Mol. Biol.* **288:** 427–439.

Burkhart, B.M. 1995. Structure of the trigonal form of recombinant oxidized flavodoxin from *Anabaena* 7120 at 1.40 Å resolution. *Acta Crystallogr. D. Biol. Crystallogr.* **51:** 318–330.

Burnett, R.M., Darling, G.D., Kendall, D.S., LeQuesne, M.E., Mayhew, S.G., Smith, W.W., and Ludwig, M.L. 1974. The structure of the oxidized form of clostridial flavodoxin at 1.9-Å resolution. *J. Biol. Chem* **249:** 4383–4392.

Chang, F.C. and Swenson, R.P. 1999. The midpoint potentials for the oxidized-semiquinone couple for Gly57 mutants of the *Clostridium beijerinckii* flavodoxin correlate with changes in the hydrogen-bonding interaction with the proton on N(5) of the reduced flavin mononucleotide cofactor as measured by NMR chemical shift temperature dependencies. *Biochemistry* **38:** 7168–7176.

Cheddar, G., Meyer, T.E., Cusanovich, M.A., Stout, C.D., and Tollin, G. 1986. Electron-transfer reactions between flavodoxin semiquinone and *c*-type cytochromes: Comparisons between various flavodoxins. *Biochemistry* **25:** 6502–6507.

Curley, G.P., Carr, M.C., Mayhew, S.G., and Voordouw, G. 1991. Redox and flavin-binding properties of recombinant flavodoxin from *Desulfovibrio vulgaris* (Hildenborough). *Eur. J. Biochem.* **202:** 1091–1100.

De Francesco, R., Tollin, G., and Edmondson, D.E. 1987. Influence of 8 α-imidazole substitution of the FMN cofactor on the rate of electron transfer from the neutral semiquinones of two flavodoxins to cytochrome *c*. *Biochemistry* **26:** 5036–5042.

Deistung, J. and Thorneley, R.N.F. 1986. Electron transfer to nitrogenase: Characterization of flavodoxin from *Azotobacter chroococcum* and comparison of its redox potentials with those of flavodoxins from *Azotobacter vinelandii* and *Klebsiella pneumoniae* (nifF gene product). *Biochem. J.* **239:** 69–75.

Drennan, C.L., Pattridge, K.A., Weber, C.H., Metzger, A.L., Hoover, D.M., and Ludwig, M.L. 1999. Refined structures of oxidized flavodoxin from *Anacystis nidulans*. *J. Mol. Biol.* **294:** 711–724.

Drummond, M.H. 1986. Structure predictions and surface charge of nitrogenase flavodoxins from *Klebsiella pneumoniae* and *Azotobacter vinelandii*. *Eur. J. Biochem.* **159:** 549–553.

Duyvis, M.G., Wassink, H., and Haaker, H. 1998. Nitrogenase of *Azotobacter vinelandii*: Kinetic analysis of the Fe protein redox cycle. *Biochemistry* **37:** 17345–17354.

Franken, H.D., Ruterjans, H., and Müller, F. 1984. Nuclear-magnetic-resonance investigation of ^{15}N-labeled flavins, free and bound to *Megasphaera elsdenii* apoflavodoxin. *Eur. J. Biochem.* **138:** 481–489.

Freigang, J., Diederichs, K., Schafer, K.P., Welte, W., and Paul, R. 2002. Crystal structure of oxidized flavodoxin, an essential protein in *Helicobacter pylori*. *Protein Sci.* **11:** 253–261.

French, S.W.K. 1978. On the treatment of negative intensity observations. *Acta Crystallogr. A* **34:** 517–524.

Fukuyama, K., Matsubara, H., and Rogers, L.J. 1992. Crystal structure of oxidized flavodoxin from a red alga *Chondrus crispus* refined at 1.8 Å resolution: Description of the flavin mononucleotide binding site. *J. Mol. Biol.* **225:** 775–789.

Hoover, D.M. and Ludwig, M.L. 1997. A flavodoxin that is required for enzyme activation: The structure of oxidized flavodoxin from *Escherichia coli* at 1.8 Å resolution. *Protein Sci.* **6:** 2525–2537.

Hoover, D.M., Drennan, C.L., Metzger, A.L., Osborne, C., Weber, C.H., Pattridge, K.A., and Ludwig, M.L. 1999. Comparisons of wild-type and mutant flavodoxins from *Anacystis nidulans*. Structural determinants of the redox potentials. *J. Mol. Biol.* **294:** 725–743.

Hutchinson, E.G. and Thornton, J.M. 1994. A revised set of potentials for β-turn formation in proteins. *Protein Sci.* **3:** 2207–2216.

Jones, T.A., Zou, J.Y., Cowan, S.W., and Kjeldgaard, M. 1991. Improved methods for building protein models in electron density maps and the location of errors in these models. *Acta Crystallogr. A* **47:** 110–119.

Kabsch, W. and Sander, C. 1983. Dictionary of Protein Secondary Structure: Pattern-recognition of hydrogen-bonded and geometrical features. *Biopolymers* **22:** 2577–2637.

Kelley, L.A., MacCallum, R.M., and Sternberg, M.J. 2000. Enhanced genome annotation using structural profiles in the program 3D-PSSM. *J. Mol. Biol.* **299:** 499–520.

Kissinger, C.R., Gehlhaar, D.K., and Fogel, D.B. 1999. Rapid automated molecular replacement by evolutionary search. *Acta Crystallogr. D. Biol. Crystallogr.* **55:** 484–491.

Klugkist, J., Haaker, H., and Veeger, C. 1986a. Studies on the mechanism of electron transport to nitrogenase in *Azotobacter vinelandii*. *Eur. J. Biochem.* **155:** 41–46.

Klugkist, J., Voorberg, J., Haaker, H., and Veeger, C. 1986b. Characterization of three different flavodoxins from *Azotobacter vinelandii*. *Eur. J. Biochem.* **155:** 33–40.

Laskowski, R.A., Moss, D.S., and Thornton, J.M. 1993. Main-chain bond lengths and bond angles in protein structures. *J. Mol. Biol.* **231:** 1049–1067.

Lopez-Llano, J., Maldonado, S., Bueno, M., Lostao, A., Angeles-Jimenez, M., Lillo, M.P., and Sancho, J. 2004a. The long and short flavodoxin: I. The role of the differentiating loop in apoflavodoxin structure and FMN binding. *J. Biol. Chem.* **279:** 47177–47183.

Lopez-Llano, J., Maldonado, S., Jain, S., Lostao, A., Godoy-Ruiz, R., Sanchez-Ruiz, J.M., Cortijo, M., Fernandez-Recio, J., and Sancho, J. 2004b. The long and short flavodoxins: II. The role of the differentiating loop in apoflavodoxin stability and folding mechanism. *J. Biol. Chem.* **279:** 47184–47191.

Lostao, A., Gómez-Moreno, C., Mayhew, S.G., and Sancho, J. 1997. Differential stabilization of the three FMN redox forms by tyrosine 94 and tryptophan 57 in flavodoxin from *Anabaena* and its influence on the redox potentials. *Biochemistry* **36:** 14334–14344.

Lostao, A., El Harrous, M., Daoudi, F., Romero, A., Parody-Morreale, A., and Sancho, J. 2000. Dissecting the energetics of the apoflavodoxin-FMN complex. *J. Biol. Chem.* **275:** 9518–9526.

Ludwig, M.L. and Luschinsky, C.L. 1992. Structure and redox properties of clostridial flavodoxin. In *Chemistry and biochemistry of flavoenzymes* (ed. F. Müller), Vol. 3, pp. 427–466. CRC Press, Boca Raton, FL.

Ludwig, M.L., Schopfer, L.M., Metzger, A.L., Pattridge, K.A., and Massey, V. 1990. Structure and oxidation-reduction behavior of 1-deaza-FMN flavodoxins: Modulation of redox potentials in flavodoxins. *Biochemistry* **29:** 10364–10375.

Ludwig, M.L., Pattridge, K.A., Metzger, A.L., Dixon, M.M., Eren, M., Feng, Y., and Swenson, R.P. 1997. Control of oxidation-reduction potentials in flavodoxin from *Clostridium beijerinckii*: The role of conformation changes. *Biochemistry* **36:** 1259–1280.

Mayhew, S.G. 1971. Studies on flavin binding in flavodoxins. *Biochim. Biophys. Acta* **235:** 289–302.

Mayhew, S.G. and Ludwig, M.L. 1975. Flavodoxins and electron-transferring flavoproteins. In *The enzymes* (ed. P.D. Boyer), Vol. 12, pp. 57–118. Academic Press, New York.

Mayhew, S.G. and Tollin, G. 1992. General properties of flavodoxins. In *Chemistry and biochemistry of flavoenzymes*, Vol. 3 (ed. F. Müller), pp. 389–426. CRC Press, Boca Raton, FL.

Mayhew, S.G., Foust, G.P., and Massey, V. 1969. Oxidation-reduction properties of flavodoxin from *Peptostreptococcus elsdenii*. *J. Biol. Chem.* **244:** 803–810.

Mayhew, S.G., O'Connell, D.P., O'Farrell, P.A., Yalloway, G.N., and Geoghegan, S.M. 1996. Regulation of the redox potentials of flavodoxins: Modification of the flavin binding site. *Biochem. Soc. Trans.* **24:** 122–127.

McCarthy, A.A., Walsh, M.A., Verma, C.S., O'Connell, D.P., Reinhold, M., Yalloway, G.N., D'Arcy, D., Higgins, T.M., Voordouw, G., and Mayhew, S.G. 2002. Crystallographic investigation of the role of aspartate 95 in the modulation of the redox potentials of *Desulfovibrio vulgaris* flavodoxin. *Biochemistry* **41:** 10950–10962.

Murshudov, G.N. 1997. Refinement of macromolecular structures by the maximum-likelihood method. *Acta Crystallogr. D. Biol. Crystallogr.* **53:** 240–255.

Otwinowski, Z. and Minor, W. 1997. Processing of X-ray diffraction data collected in oscillation mode. *Methods Enzymol.* **276:** 307–326.

Paulsen, K.E., Stankovich, M.T., Stockman, B.J., and Markley, J.L. 1990. Redox and spectral properties of flavodoxin from *Anabaena* 7120. *Arch. Biochem. Biophy.* **280:** 68–73.

Peelen, S., Wijmenga, S., Erbel, P.J., Robson, R.L., Eady, R.R., and Vervoort, J. 1996. Possible role of a short extra loop of the long-chain flavodoxin from *Azotobacter chroococcum* in electron transfer to nitrogenase: Complete ^{1}H, ^{15}N and ^{13}C backbone assignments and secondary solution structure of the flavodoxin. *J. Biomol. NMR* **7:** 315–330.

Pueyo, J.J., Curley, G.P., and Mayhew, S.G. 1996. Kinetics and thermodynamics of the binding of riboflavin, riboflavin 5′-phosphate and riboflavin 3′,5′-bisphosphate by apoflavodoxins. *Biochem J.* **313 (Pt. 3):** 855–861.

Rao, S.T., Shaffie, F., Yu, C., Satyshur, K.A., Stockman, B.J., Markley, J.L., and Sundarlingam, M. 1992. Structure of the oxidized long-chain flavodoxin from *Anabaena* 7120 at 2 Å resolution. *Protein Sci.* **1:** 1413–1427.

Romero, A., Caldeira, J., Legall, J., Moura, I., Moura, J.J., and Romao, M.J. 1996. Crystal structure of flavodoxin from *Desulfovibrio desulfuricans* ATCC 27774 in two oxidation states. *Eur. J. Biochem.* **239:** 190–196.

Smith, W.W., Burnett, R.M., Darling, G.D., and Ludwig, M.L. 1977. Structure of the semiquinone form of flavodoxin from *Clostridum* MP: Extension of 1.8 Å resolution and some comparisons with the oxidized state. *J. Mol. Biol.* **117:** 195–225.

Smith, W.W., Pattridge, K.A., Ludwig, M.L., Petsko, G.A., Tsernoglou, D., Tanaka, M., and Yasunobu, K.T. 1983. Structure of oxidized flavodoxin from *Anacystis nidulans*. *J. Mol. Biol.* **165:** 737–753.

Steensma, E., Heering, H.A., Hagen, W.R., and van Mierlo, C.P. 1996. Redox properties of wild-type, Cys69Ala, and Cys69Ser *Azotobacter vinelandii* flavodoxin II as measured by cyclic voltammetry and EPR spectroscopy. *Eur. J. Biochem.* **235:** 167–172.

Steensma, E., Nijman, M.J., Bollen, Y.J., de Jager, P.A., van den Berg, W.A., van Dongen, W.M., and van Mierlo, C.P. 1998. Apparent local stability of the secondary structure of *Azotobacter vinelandii* holoflavodoxin II as probed by hydrogen exchange: implications for redox potential regulation and flavodoxin folding. *Protein Sci.* **7:** 306–317.

Stockman, B.J., Westler, W.M., Mooberry, E.S., and Markley, J.L. 1988. Flavodoxin from *Anabaena* 7120: Uniform nitrogen-15 enrichment and hydrogen-1, nitrogen-15, and phosphorus-31 NMR investigations of the flavin mononucleotide binding site in the reduced and oxidized states. *Biochemistry* **27:** 136–142.

Swenson, R.P. and Krey, G.D. 1994. Site-directed mutagenesis of tyrosine-98 in the flavodoxin from *Desulfovibrio vulgaris* (Hildenborough): Regulation of oxidation-reduction properties of the bound FMN cofactor by aromatic, solvent, and electrostatic interactions. *Biochemistry* **33:** 8505–8514.

Sykes, G.A. and Rogers, L.J. 1984. Redox potentials of algal and cyanobacterial flavodoxins. *Biochem. J.* **217:** 845–850.

Taylor, M.F., Boylan, M.H., and Edmondson, D.E. 1990. *Azotobacter vinelandii* flavodoxin: Purification and properties of the recombinant, dephospho form expressed in *Escherichia coli*. *Biochemistry* **29:** 6911–6918.

Thompson, J.D., Higgins, D.G., and Gibson, T.J. 1994. CLUSTAL W: Improving the sensitivity of progressive multiple sequence alignment through sequence weighting, position-specific gap penalties and weight matrix choice. *Nucleic Acids Res.* **22:** 4673–4680.

Thorneley, R.N.F., Ashby, G.A., Drummond, M.H., Eady, R.R., Hughes, D.L., Ford, G., Harrison, P.M., Shaw, A., Robson, R.L., Kazlauskaite, J., et al. 1994. Flavodoxins and nitrogen fixation: Structure, electrochemistry and post-translational modification by coenzyme A. In *Flavins and flavoproteins*, pp. 343–354. Walter de Gruyter, Berlin.

Tollin, G. and Edmondson, D.E. 1980. Purification and properties of flavodoxins. *Methods Enzymol.* **69:** 392–406.

van Mierlo, C.P., Lijnzaad, P., Vervoort, J., Müller, F., Berendsen, H.J., and de Vlieg, J. 1990. Tertiary structure of two-electron reduced *Megasphaera elsdenii* flavodoxin and some implications, as determined by two-dimensional ^{1}H-NMR and restrained molecular dynamics. *Eur. J. Biochem.* **194:** 185–198.

van Mierlo, C.P., van Dongen, W.M., Vergeldt, F., van Berkel, W.J., and Steensma, E. 1998. The equilibrium unfolding of *Azotobacter vinelandii* apoflavodoxin II occurs via a relatively stable folding intermediate. *Protein Sci.* **7:** 2331–2344.

van Mierlo, C.P., van den Oever, J.M., and Steensma, E. 2000. Apoflavodoxin (un)folding followed at the residue level by NMR. *Protein Sci.* **9:** 145–157.

Vervoort, J., van Berkel, W.J., Mayhew, S.G., Müller, F., Bacher, A., Nielsen, P., and LeGall, J. 1986. Properties of the complexes of riboflavin 3′,5′-bisphosphate and the apoflavodoxins from *Megasphaera elsdenii* and *Desulfovibrio vulgaris*. *Eur. J. Biochem.* **161:** 749–756.

Watt, W., Tulinsky, A., Swenson, R.P., and Watenpaugh, K.D. 1991. Comparison of the crystal structures of a flavodoxin in its three oxidation states at cryogenic temperatures. *J. Mol. Biol.* **218:** 195–208.

Yoch, D.C. 1975. Dimerization of *Azotobacter vinelandii* flavodoxin (azotoflavin). *Arch. Biochem. Biophys.* **170:** 326–333.

Zhou, Z., and Swenson, R.P. 1995. Electrostatic effects of surface acidic amino acid residues on the oxidation-reduction potentials of the flavodoxin from *Desulfovibrio vulgaris* (Hildenborough). *Biochemistry* **34:** 3183–3192.

———. 1996a. Evaluation of the electrostatic effect of the 5′-phosphate of the flavin mononucleotide cofactor on the oxidation–reduction potentials of the flavodoxin from *Desulfovibrio vulgaris* (Hildenborough). *Biochemistry* **35:** 12443–12454.

———. 1996b. The cumulative electrostatic effect of aromatic stacking interactions and the negative electrostatic environment of the flavin mononucleotide binding site is a major determinant of the reduction potential for the flavodoxin from *Desulfovibrio vulgaris* (Hildenborough). *Biochemistry* **35:** 15980–15988.